An interactive spatial compartment model for oral delivery of biologics to the colon

Pierre BAUËR and Bilal MAZHAR

Plantibodies

pierre.bauer@plantibodies.tech

Exploratory computational manuscript — not submitted

Abstract

Background. Oral local delivery of biologics to the colon requires protection, release and access to the target-containing tissue. We describe an interactive, one-dimensional, spatial compartment simulator for a plant-derived anti-tumour necrosis factor (TNF) antibody formulation. **Methods.** The colon was represented by 20 axial segments, each containing protected luminal antibody, free luminal antibody, mucus, epithelial endosomal and cytosolic pools, lamina propria and an abstract target-bound pool. Lymphoid tissue, lymph nodes and plasma were represented as pooled compartments. Four hypothetical adjunct scenarios were calculated using the simulator code. A nominal 10 mg dose every 12 h and a 70% active arrival fraction were assumed. All transport and binding parameters were hypothetical. **Results.** For the illustrative 150 kDa baseline, free-antibody amount–time integrals in one distal lamina-propria segment over 96 h were 0.147, 0.270, 0.164 and 0.284 mg h for neither adjunct, a cell-penetrating peptide (CPP), a generic paracellular enhancer, and both, respectively. Peak pooled plasma amounts were 0.0122, 0.0227, 0.0158 and 0.0258 mg. The maximum mass-balance residual was 8.9×10^{-13} mg. These outputs reflect assumed parameters, not experimental or clinical observations. **Conclusions.** The model supports transparent scenario analysis and experimental planning. Numerical refinement, formulation-specific data and independent biological validation are required before quantitative or clinical application.

Keywords: oral biologics; colon; anti-TNF; mathematical modeling; compartment model; permeation enhancement.

1 Introduction

Biologics targeting TNF can treat inflammatory bowel disease, but oral local delivery presents independent challenges of upper-gastrointestinal protection, release of active material, mucosal transport and target engagement. A small study of an engineered oral anti-TNF domain antibody reported intestinal recovery and evidence consistent with mucosal activity [1]. That construct and formulation differ from the full-size antibody considered here. A mouse pharmacokinetic model has similarly emphasized tissue target engagement, but its parameter values cannot be directly transferred to human oral delivery [2].

A plant-derived powder formulation is considered as a developer-supplied design concept. The stated dose is 1 g of dried plant powder containing 10 mg of an adalimumab-like antibody, placed in an enteric capsule. No capsule dissolution, upper-gastrointestinal survival, release, plant-matrix

composition or functional activity measurements are available for this study. The capsule is intended to reduce gastric exposure; colon-specific opening has not been demonstrated. The source plant and process details are intentionally not disclosed here. The objective is to describe and verify the implemented simulator and to illustrate how assumptions about mucosal transport and adjuncts affect its outputs. This is not a qualified physiologically based pharmacokinetic model or a tool for choosing a clinical dose.

2 Methods

2.1 Model structure and state variables

The model approximates a colon of length $L = 1.5$ m using $N = 20$ equal segments, indexed by $i = 1, \ldots, N$ with $\Delta x = L/N$. The states E_i, L_i, M_i, I_i, Y_i, T_i and B_i denote protected active protein, free active luminal protein, mucus-associated protein, epithelial endosomal protein, epithelial cytosolic protein, free lamina-propria protein and an abstract bound pool, respectively. Each is an amount in mg, not a concentration. The symbol L_i denotes a state and is distinct from the length L. Colonic lymphoid tissue G, draining lymph nodes Q, plasma P and lymphoid bound material B_G are pooled amounts in mg. A dimensionless auxiliary variable S_i represents local enhancer exposure, not the mass or concentration of a named ingredient. Figure 1 presents a simplified network.

The model clock begins at the arrival of the first dose at the colon. At times $t_n = 12n$ h for $n = 0, \ldots, 7$, protected mass $q = f_{\text{arr}} D$ is added equally to segments 1 and 2, where $D = 10$ mg and $f_{\text{arr}} = 0.70$ for the baseline. Thus $q = 7$ mg is assumed to arrive at each event. This is a scenario assumption, not a measurement of the capsule or powder. When the enhancer is enabled, an arbitrary signal of 0.5 units is also added to each of the first two segments at each event. No pre-colonic compartment is simulated.

2.2 Axial transport and release

The protected and free luminal amounts are governed by

$$\dot{E}_i = \mathcal{A}_i(E) - k_r E_i + u_i(t), \tag{1}$$

$$\dot{L}_i = \mathcal{A}_i(L) + \mathcal{D}_i(L) + k_r E_i - a_{LM} L_i + a_{ML} M_i - k_L L_i - \beta_i^L, \tag{2}$$

where the bolus input $u_i(t)$ is implemented as an instantaneous event, $k_r = \ln 2/8$ h^{-1} and $k_L = \ln 2/12$ h^{-1} at baseline. Upwind advection and centered dispersion are

$$\mathcal{A}_i(X) = \frac{v}{\Delta x}(X_{i-1} - X_i), \tag{3}$$

$$\mathcal{D}_i(L) = \frac{D_x}{\Delta x^2}(L_{i-1} - 2L_i + L_{i+1}), \tag{4}$$

with $v = L/24$ m h^{-1} and $D_x = 0.002$ m^2 h^{-1}. For advection the upstream state is zero; distal advective flow is an excretion sink. For dispersion, ghost states equal the adjacent boundary state, giving zero diffusive flux at both ends. Protected material has no explicit physical dispersion or degradation in this model.

2.3 Mucosal exchange and target binding

With all rate constants in h^{-1}, the local tissue equations are

$$\dot{M}_i = a_{LM}L_i - a_{ML}M_i - a_{MI}M_i - a_{MT,i}M_i + a_{TM}T_i - k_M M_i - \beta_i^M, \tag{5}$$

$$\dot{I}_i = a_{MI}M_i - a_{IT,i}I_i - k_e I_i - k_I I_i, \tag{6}$$

$$\dot{Y}_i = k_e I_i - k_Y Y_i - \beta_i^Y, \tag{7}$$

$$\dot{T}_i = a_{MT,i}M_i + a_{IT,i}I_i - (a_{TM} + a_{TG} + a_{TQ} + a_{TP} + k_{T,i})T_i - \beta_i^T. \tag{8}$$

For a protein mass m in kDa the implemented heuristic is

$$s(m) = \mathrm{clip}\Big[(150/m)^{1/3},\, 0.2,\, 3\Big], \tag{9}$$

where clipping limits the factor to the indicated interval. This is an illustrative sensitivity rule, not a measured molecular-size relationship. The nominal exchange coefficients are $a_{LM} = 0.10s$, $a_{ML} = 0.10$, $a_{MI} = 0.015s\, m_{\mathrm{CPP}}$, $a_{MT,i} = 0.001s\, m_{P,i}$, $a_{IT,i} = 0.015 m_{T,i}$, $a_{TM} = 0.02$, $a_{TG} = 0.002$, $a_{TQ} = 0.01$ and $a_{TP} = 0.003$. The nominal inactivation coefficients are $k_M = 0.06$, $k_I = 0.15$, $k_Y = 0.05$ and $k_{T,i} = 0.04$; the endosomal escape rate is $k_e = 0.02$. The default CPP-on setting uses $m_{\mathrm{CPP}} = 3$, compared with 1 when off. It changes uptake into I only. These states are phenomenological and cannot establish a particular molecule's intracellular delivery.

The selected target compartment uses a dimensionless selector $\chi_j \in \{0, 1\}$, with at most one active target location among luminal, mucus-associated, epithelial cytosolic and lamina-propria pools. For the selected state X_i^j,

$$b_i^+ = k_{\mathrm{on}} X_i^j \max\left(0, 1 - \frac{B_i}{B_{\max}}\right), \qquad b_i^- = k_{\mathrm{off}} B_i, \tag{10}$$

$$\dot{B}_i = b_i^+ - b_i^-, \qquad \beta_i^j = \chi_j (b_i^+ - b_i^-). \tag{11}$$

Here $k_{\mathrm{on}} = 0.1\ \mathrm{h}^{-1}$, $k_{\mathrm{off}} = 0.02\ \mathrm{h}^{-1}$ and $B_{\max} = 0.1/N$ mg. If no local target is selected, local binding is disabled. This is an abstract capacity-limited mass rule: target turnover, target concentration, antibody valency and free TNF are absent. It is not a TNF-neutralization prediction. For the lymphoid-target option the same binding rule applies to G and B_G with $B_{G,\max} = 0.1$ mg; local binding is disabled.

2.4 Enhancer, inflammatory regions and pooled compartments

The enhancer signal and local multiplier are

$$\dot{S}_i = \mathcal{A}_i(S) - \frac{\ln 2}{h_S} S_i + w_i(t), \tag{12}$$

$$\phi_i = 1 + (m_{\max} - 1)\frac{S_i}{0.1 + S_i}, \tag{13}$$

where $h_S = 4$ h and $m_{\max} = 5$ in the illustrative runs, and w_i denotes the dose-linked signal pulses. With a paracellular scenario, $m_{P,i} = \phi_i$ and $m_{T,i} = 1$; with a transcellular scenario, $m_{P,i} = 1$ and $m_{T,i} = \phi_i$; both are 1 when no enhancer is present. The CPP and enhancer terms combine algebraically; no specific molecular interaction or synergistic mechanism is modeled. Existing epithelial transport and enhancer studies motivate separating uptake from barrier transport, but do not supply these coefficients for the present formulation [3, 4, 5].

A user-selectable hypothetical inflammatory region multiplies $a_{MT,i}$ by 2 and $k_{T,i}$ by 1.5 in affected segments. It does not simulate an actual inflammatory response, patient phenotype or calibrated disease severity. No region was modified in the main comparisons. The pooled mass balances are

$$\dot{G} = a_{TG} \sum_i T_i - (0.02 + 0.03)G - \beta_G, \tag{14}$$

$$\dot{Q} = a_{TQ} \sum_i T_i + 0.02G - (0.04 + 0.02)Q, \tag{15}$$

$$\dot{P} = a_{TP} \sum_i T_i + 0.04Q - 0.03P, \tag{16}$$

where β_G is the lymphoid binding flux when that target is selected and zero otherwise. The terms $0.03G$, $0.02Q$ and $0.03P$ are loss fluxes. These pathways are placeholders: lymphoid follicles, lymph nodes and systemic circulation are not spatially resolved.

2.5 Numerical scheme, scenarios and endpoints

The coupled balances are advanced using explicit Euler with $\Delta t = 0.025$ h for 96 h and sampled every 0.5 h. The simulator can vary the assumed arrival fraction, release half-life, protein size, target location, adjunct settings and regional disease scenario. Figure 2 uses a 150 kDa protein, arrival fraction 0.70, release half-life 8 h, no modified region and lamina-propria target. Four runs were made by turning the CPP and the paracellular enhancer independently on or off. For each, the endpoint was free lamina-propria mass in zero-based segment 15 and pooled plasma mass; the trapezoidal rule was applied to sampled values for the 0–96 h segment mass–time integral. These are not concentrations or a tissue-to-plasma ratio.

The cumulative mass check is

$$M_{\text{in}} = \sum_i (E_i + L_i + M_i + I_i + Y_i + T_i + B_i) + G + Q + P + B_G + M_{\text{loss}} + M_{\text{out}}, \tag{17}$$

where M_{loss} accumulates the specified inactivation terms and M_{out} is distal advection. This check tests accounting only. First-order upwind advection causes numerical dispersion. For the baseline, its leading-order estimate [7] is

$$D_{\text{num}} \simeq \frac{v\Delta x}{2}\left(1 - \frac{v\Delta t}{\Delta x}\right) \simeq 0.00229 \text{ m}^2\,\text{h}^{-1}, \tag{18}$$

which is comparable to the prescribed D_x. The estimate concerns the advection discretization; it is not a substitute for convergence analysis of the coupled model. As a result, spatial profiles require grid and time-step refinement before quantitative use.

3 Results

The 0–96 h integrals of free lamina-propria mass in distal segment 15 were 0.147, 0.270, 0.164 and 0.284 mg h for neither adjunct, CPP only, enhancer only and both, respectively. At 72 h, the corresponding masses were 0.00246, 0.00460, 0.00272 and 0.00482 mg. Peak pooled plasma amounts were 0.0122, 0.0227, 0.0158 and 0.0258 mg (Figure 2). The computed differences are consequences of the stipulated equations and coefficients, not measurements of the formulation or estimates of treatment effect.

Across the four simulations, the maximum absolute residual in Eq. (17) was 8.9×10^{-13} mg. Sampled aggregate and selected-segment outputs were non-negative. This verifies accounting for these particular runs but does not establish physiological validity, convergence or performance under all permitted inputs.

4 Discussion

The simulator combines axial delivery with schematic local compartments to support comparison of explicit assumptions. Its three-dimensional colon image is a visual projection of a one-dimensional calculation. The white marker selects an axial segment for the cross-section and comparison plot; it does not redirect the dose. Colonic lymphoid tissue, nodes and plasma are pooled, and the modeled epithelial endosomal and cytosolic pools should not be interpreted as direct imaging or independent biological measurements.

The comparison is a hypothesis-generating demonstration. It cannot show that a CPP increases delivery of the specific antibody, that an enhancer is safe in inflamed tissue, or that any modeled binding corresponds to TNF neutralization. Epithelial transport and barrier responses vary with formulation and context [3, 4, 5]. Regional distribution in ulcerative colitis is also heterogeneous; published transit data for a different formulation do not determine the present model's rate constants [6]. The user-defined protein-size factor, dose arrival fraction, release, losses, exchange, enhancer signal, target capacity and inflammation multipliers all lack calibration. In particular, the size rule and binding equation are not derived from diffusion theory or antigen kinetics.

Several numerical and structural limitations constrain interpretation. The upwind method adds substantial numerical dispersion, especially on the present grid. Mucus is a single pool, the colon has uniform geometry, the delivery carrier is reduced to a lumped protected mass, and compartment volumes, local fluid heterogeneity and separate soluble versus membrane TNF dynamics are absent. Blood and lymph estimates rely on arbitrary rates. Per-segment amounts cannot be used to calculate concentrations without a defensible compartment volume, and choosing a smaller value for a hypothetical volume would not itself validate exposure. The graphical cross-section is schematic rather than a resolved radial transport calculation.

A staged research program should quantify batch-level total and functional antibody, recovery after sequential simulated gastrointestinal exposure, and time-resolved release under relevant colonic conditions. Free-protein inactivation should be measured separately. CPP and enhancer comparisons should quantify functional protein movement, tissue distribution, barrier function, viability and recovery using independent controls and complementary assays. Training and independent evaluation datasets should be separated. Once suitable measurements are available, uncertainty, parameter identifiability, model alternatives and grid/time refinement should be assessed. Human experiments require independent ethical and regulatory review. The principles of model evaluation and documentation in the ICH M15 guidance are relevant to planning, but this model is not represented as qualified for regulatory use [8].

5 Conclusions

This exploratory simulator makes the relationship between chosen delivery assumptions and computed amounts explicit. Its outputs do not demonstrate human exposure, efficacy, safety or target engagement. Formulation-specific measurements and independent numerical and biological validation are necessary before use beyond hypothesis generation.

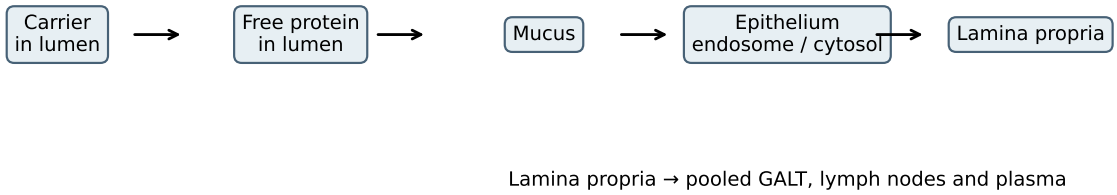


Figure 1: Simplified simulator structure. Axial segments contain local protected, free, mucus, epithelial and lamina-propria pools. Lymphoid tissue, lymph nodes and plasma are pooled. Loss, back-transfer and generic binding are defined in the equations.

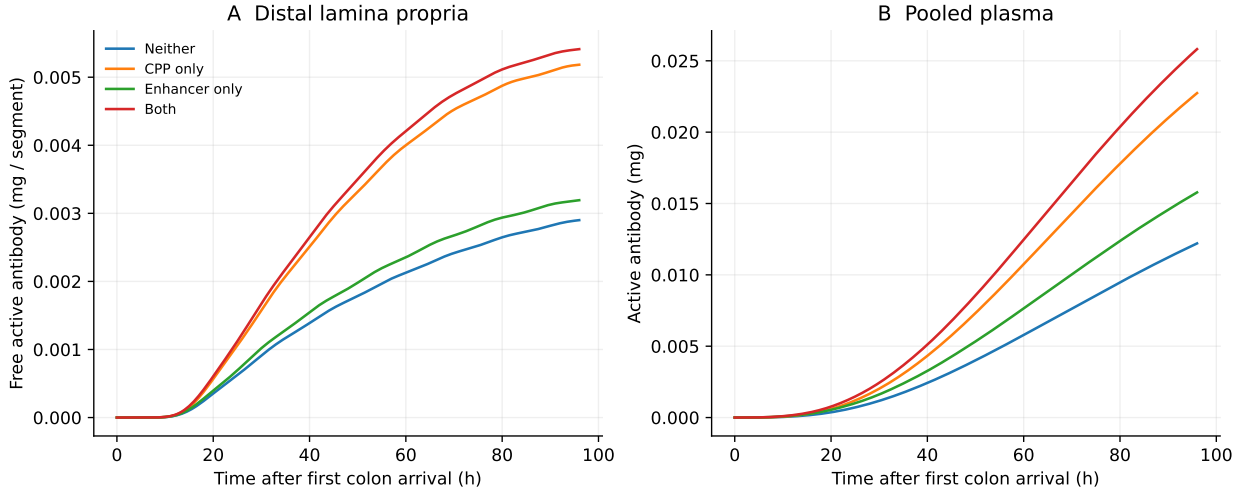


Figure 2: Illustrative outcomes generated directly from the simulator. (A) Free active antibody amount in distal lamina-propria segment 15. (B) Pooled active plasma amount. All adjunct and transport coefficients are hypothetical; no experimental data or confidence intervals are shown.

References

[1] Nurbhai S, Roberts KJ, Carlton TM, et al. Oral anti-tumour necrosis factor domain antibody V565 provides high intestinal concentrations, and reduces markers of inflammation in ulcerative colitis patients. *Sci Rep*. 2019;9:14042. doi:10.1038/s41598-019-50545-x.

[2] Zheng S, Niu J, Geist B, et al. A minimal physiologically based pharmacokinetic model to characterize colon TNF suppression and treatment effects of an anti-TNF monoclonal antibody in a mouse inflammatory bowel disease model. *mAbs*. 2020;12:1813962. doi:10.1080/19420862.2020.1813962.

[3] Kamei N, Onuki Y, Takayama K, Takeda-Morishita M. Mechanistic study of the uptake/permeation of cell-penetrating peptides across a Caco-2 monolayer and their stimulatory effect on epithelial insulin transport. *J Pharm Sci*. 2013;102:3998–4008. doi:10.1002/jps.23708.

[4] Kamei N, Aoyama Y, Khafagy ES, Henmi M, Takeda-Morishita M. Effect of different intestinal conditions on the intermolecular interaction between insulin and cell-penetrating peptide penetratin and on its contribution to stimulation of permeation through intestinal epithelium. *Eur J Pharm Biopharm*. 2015;94:42–51. doi:10.1016/j.ejpb.2015.04.030.

[5] Twarog C, Liu K, O'Brien PJ, et al. A head-to-head Caco-2 assay comparison of the mechanisms of action of the intestinal permeation enhancers SNAC and sodium caprate. *Eur J Pharm Biopharm*. 2020;152:95–107. doi:10.1016/j.ejpb.2020.04.023.

[6] Hebden JM, Blackshaw PE, Perkins AC, et al. Limited exposure of the healthy distal colon to orally-dosed formulation is further exaggerated in active left-sided ulcerative colitis. *Aliment Pharmacol Ther*. 2000;14:155–161. doi:10.1046/j.1365-2036.2000.00697.x.

[7] US Army Corps of Engineers. CE-QUAL-W2 documentation: Numerical solution. https://ce-qual-w2-erdc.github.io/cequalw2-docs/part2/05_numerical_solution/. Accessed 2 November 2026.

[8] US Food and Drug Administration. M15 General Principles for Model-Informed Drug Development. Final guidance. https://www.fda.gov/regulatory-information/search-fda-guidance-documents/m15-general-principles-model-informed-drug-development. Accessed 2 November 2026.